

# Mechanistic Studies on the Reactions of Molybdenum(VI), Tungsten(VI), Vanadium(V), and Arsenic(V) Tetraoxo Anions with the Fe<sup>II</sup>Fe<sup>III</sup> Form of Purple Acid Phosphatase from Porcine Uteri (Uteroferrin)

Joo-Sang Lim, Manuel A. S. Aquino, and A. Geoffrey Sykes\*

Department of Chemistry, The University of Newcastle, Newcastle upon Tyne NE1 7RU, England, U.K.

Received February 9, 1995<sup>⊗</sup>

The Fe<sup>II</sup>Fe<sup>III</sup> form of purple acid phosphatase (PAP<sub>r</sub>) from porcine uteri (uteroferrin) catalyses the hydrolysis of phosphate esters. In a previous paper kinetic studies on the reactions of PAP<sub>r</sub> with five different phosphate moieties, including [H<sub>2</sub>PO<sub>4</sub>]<sup>-</sup> as a prototype, were reported. Here these studies have been extended to include the complexing of tetraoxo XO<sub>4</sub> anions of molybdate(VI), tungstate(VI), vanadate(V), and arsenate(V) with PAP<sub>r</sub>. UV-vis absorbance changes are small and the range of concentrations is restricted by the need to maximise monomer XO<sub>4</sub> forms. Rate constants *k*<sub>obs</sub>(25 °C) were determined by stopped-flow monitoring of the reactions at ~520 nm. Absorbance changes with arsenate(V) were too small for rate constants to be evaluated. At pH 5.6 the *k*<sub>obs</sub> values obtained are independent of [XO<sub>4</sub>] (X = Mo, W, V), in the range (0.4–10) × 10<sup>-4</sup> M. At concentrations of VO<sub>4</sub> > 2.0 × 10<sup>-4</sup> M formation of [V<sub>3</sub>O<sub>9</sub>]<sup>3-</sup> occurs, and a decrease in experimentally determined rate constants is observed. In the pH range 3.5–6.3, as in the case of the PO<sub>4</sub> reagents, rate constants decrease with increasing pH due to the slower reaction of Fe(III)–OH as compared to Fe(III)–OH<sub>2</sub>. A mechanism involving rapid XO<sub>4</sub> binding at the more labile Fe(II) is proposed. Slower [XO<sub>4</sub>]-independent bridging to the Fe(III) then occurs with displacement of H<sub>2</sub>O at the lower pH's. Nucleophilic attack of the conjugate-base Fe(III)–OH on the phosphate-ester results in hydrolysis which peaks at pH 4.9. At this pH rate constants/s<sup>-1</sup> are for [MoO<sub>4</sub>]<sup>2-</sup> (1.33), [WO<sub>4</sub>]<sup>2-</sup> (0.77) and [H<sub>2</sub>VO<sub>4</sub>]<sup>-</sup> (1.44), as compared to values of ~0.5s<sup>-1</sup> for the five different phosphates. There is therefore little dependence on the identity of XO<sub>4</sub>. With O<sub>2</sub> the PAP<sub>r</sub>•MoO<sub>4</sub> adduct is less reactive than PAP<sub>r</sub>, while PAP<sub>r</sub>•AsO<sub>4</sub> is more reactive. These results are explained by the effect of coordinated XO<sub>4</sub> on the PAP<sub>o</sub>/PAP<sub>r</sub> reduction potential.

## Introduction

To date mammalian purple acid phosphatases (PAP) from porcine uteri and from beef spleen (M<sub>r</sub>~35 kDa) are the most extensively studied and well characterised proteins of this kind. The enzyme has a binuclear Fe site and a single polypeptide chain (318 amino acids).<sup>1</sup> The Fe<sup>II</sup>Fe<sup>III</sup> form, PAP<sub>r</sub>, catalyses the hydrolysis of phosphate esters (eq 1).<sup>2–6</sup> The intense



absorbance of the active pink Fe<sup>II</sup>Fe<sup>III</sup> form, peak at 515nm ( $\epsilon = 4000 \text{ M}^{-1}\text{cm}^{-1}$ ), and the inactive purple Fe<sup>III</sup>Fe<sup>III</sup> form, PAP<sub>o</sub>, peak at 550nm ( $\epsilon = 4000 \text{ M}^{-1}\text{cm}^{-1}$ ),<sup>7,8</sup> are due to tyrosine (phenolate) to Fe(III) ligand to metal charge-transfer (LMCT).<sup>5,9</sup> Small but perceptible changes in visible range spectra are observed on coordination of PO<sub>4</sub> or other XO<sub>4</sub> anions to PAP<sub>r</sub>.

Physical techniques including EXAFS, NMR, and EPR have been applied to better understand the active site of the mammalian enzyme.<sup>10–23</sup> It has been suggested that there is one histidine to each Fe and carboxylate coordination of Asp or Glu residues.<sup>10–16</sup> In addition an H<sub>2</sub>O is coordinated to each Fe,<sup>17,18</sup> and from EXAFS studies on the PAP<sub>o</sub>•PO<sub>4</sub> adduct evidence has been obtained for a bridging phosphate.<sup>19</sup> How-

<sup>⊗</sup> Abstract published in *Advance ACS Abstracts*, December 15, 1995.

- (1) Hunt, D. F.; Yates, J. R., III; Shabonowitz, J.; Zhu, N.-Z.; Zirino, T.; Averill, B. A.; Daurat-Larroque, S. T.; Shewale, J. G.; Roberts, R. M.; Brew, K. *Biochem. Biophys. Res. Commun.* **1987**, *144*, 1154.
- (2) Vincent, J. B.; Olivier-Lilley, G. L.; Averill, B. A. *Chem. Rev.* **1990**, *90*, 1447.
- (3) Antanaitis, B. C.; Aisen, P. *J. Biol. Chem.* **1984**, *259*, 2066.
- (4) Buih, W. C.; Bazer, F. W.; Ducsay, C.; Chun, P. W.; Roberts, R. M. *Fed. Proc. Am. Soc. Exp. Biol.* **1979**, *38*, 733.
- (5) Davis, J. C.; Averill, B. A. *Proc. Natl. Acad. Sci. U.S.A.* **1982**, *79*, 4623.
- (6) Antanaitis, B. C.; Aisen, P. *J. Biol. Chem.* **1982**, *257*, 1855.
- (7) Pyrz, J. W.; Sage, J. T.; Debrunner, D. G.; Que, L., Jr. *J. Biol. Chem.* **1986**, *261*, 11015.
- (8) Wilkins, R. G. *Chem. Soc. Rev.* **1992**, *21*, 171.
- (9) Beck, J. L.; Keough, D. T.; De Jersey, J.; Zerner, B. *Biochim. Biophys. Acta* **1984**, *791*, 357.
- (10) Kauzlarich, S. M.; Teo, B. K.; Burmann, S.; Davis, J. C.; Averill, B. A. *Inorg. Chem.* **1986**, *25*, 2781.

- (11) Wang, Z.; Ming, L.-J.; Que, L., Jr.; Vincent, J. B.; Crowder, M. W.; Averill, B. A. *Biochemistry* **1992**, *31*, 5263.
- (12) Holz, R. C.; Que, L., Jr.; Ming, L.-J. *J. Am. Chem. Soc.* **1992**, *119*, 4434.
- (13) Lauffer, R. B.; Antanaitis, B. C.; Aisen, P.; Que, L., Jr. *J. Biol. Chem.* **1983**, *258*, 14212.
- (14) Scarrow, R. C.; Pyrz, J. W.; Que, L., Jr. *J. Am. Chem. Soc.* **1990**, *112*, 657.
- (15) Antanaitis, B. C.; Peisach, J.; Mims, W. B.; Aisen, P. *J. Biol. Chem.* **1985**, *260*, 4572.
- (16) Crowder, M. W.; Vincent, J. B.; Averill, B. A. *Biochemistry* **1992**, *31*, 9603.
- (17) Doi, K.; McCracken, J.; Peisach, J.; Aisen, P. *J. Biol. Chem.* **1988**, *263*, 5757.
- (18) Wang, D. L.; Holz, R. C.; David, S. S.; Que, L., Jr.; Stankovich, M. T. *Biochemistry* **1991**, *30*, 8187.
- (19) True, A. E.; Scarrow, R. C.; Randell, C. R.; Holz, R. C.; Que, L., Jr. *J. Am. Chem. Soc.* **1993**, *115*, 4246.
- (20) Averill, B. A.; Davis, J. C.; Burmann, S.; Zirino, T.; Sanders-Loehr, J.; Loehr, T. M.; Sage, J. T.; Debrunner, P. G. *J. Am. Chem. Soc.* **1987**, *109*, 3760.
- (21) Beck, J. L.; McConachie, L. A.; Summers, A. C.; Arnold, W. N.; De Jersey, J.; Zerner, B. *Biochim. Biophys. Acta* **1986**, *869*, 61.
- (22) Day, E. P.; David, S. S.; Peterson, J.; Dunham, W. R.; Bonvoisin, J. J.; Sands, R. M.; Que, L., Jr. *J. Biol. Chem.* **1988**, *263*, 15561.
- (23) (a) Dietrich, M.; Munstermann, D.; Suerbaum, H.; Witzel, H. *Eur. J. Chem.* **1991**, *199*, 105. (b) Suerbaum, H.; Korner, M.; Witzel, H.; Atthaus, E.; Mosel, B.-D.; Muller-Warmuth, W. *Eur. J. Chem.* **1993**, *214*, 313.
- (24) Mueller, E. G.; Crowder, M. W.; Averill, B. A.; Knowles, J. R. *J. Am. Chem. Soc.* **1993**, *115*, 2974.

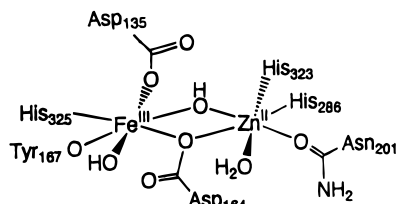
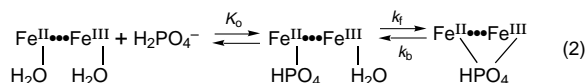


**Figure 1.** Zn<sup>II</sup>/Fe<sup>III</sup> active site structure of kidney bean purple acid phosphatase,<sup>25</sup> as a model for the Fe<sup>II</sup>/Fe<sup>III</sup> active site of the mammalian enzyme.

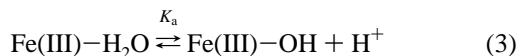
ever magnetic susceptibility measurements,<sup>5,20–22</sup> do not provide unequivocal evidence for either Fe–O–Fe (in PAP<sub>o</sub>) or Fe–OH–Fe (in PAP<sub>r</sub>). Also relevant are recent studies on the reaction of labeled adenosine 5′-triphosphate (ATP) with PAP<sub>r</sub>, which have demonstrated that transfer of phosphate to an H<sub>2</sub>O position on PAP<sub>r</sub> occurs with inversion at the phosphorus.<sup>24</sup>

There is as yet no X-ray crystal structure of the mammalian enzyme. However the structure of kidney bean phosphatase (M<sub>r</sub> ~ 55 kDa per homodimer), which has a Zn<sup>II</sup>/Fe<sup>III</sup> active site, has recently been determined at a resolution of 2.9 Å.<sup>25</sup> The Zn(II) and Fe(III) separation is 3.1 Å, and the metals are bridged by a single O-atom of the carboxylate of Asp-164. A terminal hydroxo ligand (to Fe), terminal aqua (to Zn), as well as a μ-hydroxo bridge have been modeled into the active site structure, Figure 1. When Zn is exchanged for Fe the active site shows spectroscopic behavior nearly identical to the mammalian enzyme,<sup>21,23b</sup> and similarities of the active sites are indicated. However there are also some differences,<sup>25</sup> and the functional relationship between the kidney bean and mammalian enzymes remains to be established.

An unexpected finding from kinetic studies on the reactions of PAP<sub>r</sub> (uteroferin) with five different phosphates [H<sub>2</sub>PO<sub>4</sub>]<sup>−</sup>, phenyl phosphate (and the *p*-nitro derivative), pyrophosphate, triphosphate, and adenosine 5′-triphosphate (ATP), is the observation that first-order rate constants for the uniphase processes are independent of [PO<sub>4</sub>].<sup>26</sup> Particularly relevant in the present case is the study with [H<sub>2</sub>PO<sub>4</sub>]<sup>−</sup>, which can be regarded as a prototype reaction with no associated hydrolysis step. At pH's in the range 2.6–6.5 the reaction can be summarized by eq 2, where K<sub>0</sub> is believed to involve substitution



at the more labile Fe(II), and forward and back rate constants  $k_f$  and  $k_b$  for bridge closure are as defined. At pH < 3.5 Fe(III)–H<sub>2</sub>O is present at the active site and PO<sub>4</sub> bridging ( $k_f$ ) with displacement of H<sub>2</sub>O is observed. At higher pH's as the build-up of Fe(III)–OH becomes more extensive (eq 3), and



there is a slowing down in PO<sub>4</sub> bridge closure due to the greater difficulty in displacing the hydroxide. However from activity measurements the hydrolysis of O<sub>3</sub>P(OR)<sup>2−</sup> increases due to the more extensive participation of Fe(III)–OH, consistent with a mechanism involving nucleophilic attack on the phosphate by the coordinated hydroxide.<sup>26</sup> The latter activity can be studied by monitoring absorbance changes due to the release of ROH = α-naphthol or *p*-nitrophenol from the phosphate

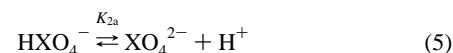
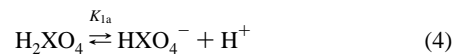
esters O<sub>3</sub>P(OR)<sup>2−</sup>, and maximizes at pH 4.9 which we believe corresponds to the maximum buildup of Fe(III)–OH. At higher pH values the enzymic activity decreases presumably because of other effects of pH, e.g. on amino acids. In the present work the tetraoxo-anions XO<sub>4</sub>, (X = Mo, W, V) and As,<sup>7,12–15</sup> are considered, with the aim of elaborating/establishing further the mechanism.<sup>23,26</sup> Recent kinetic investigations on the oxidation of PAP<sub>r</sub> to PAP<sub>o</sub> with [Fe(CN)<sub>6</sub>]<sup>3−</sup> have provided evidence for association of anionic complexes within electron-transfer range of the active site.<sup>27</sup> In other studies the effect of replacing the Fe(II) of uteroferin with Zn(II) has been explored, when the reaction with [HPO<sub>4</sub>]<sup>2−</sup> at pH 4.9 is ~35-fold faster.<sup>28</sup>

At pH 4.9 both molybdate(VI) and tungstate(VI) act as strong inhibitors for the hydrolysis of *p*-nitrophenyl phosphate by PAP<sub>r</sub> uteroferin ( $K_i$ 's both 4 μM), whereas arsenate is a weaker inhibitor ( $K_i$  = 2–15 mM).<sup>29</sup> In the present work a limiting factor is the tendency of XO<sub>4</sub> anions to oligomerize at the lower pH values, and the need to control conditions so as to maintain monomeric XO<sub>4</sub> forms as the dominant species. Effects which two of the XO<sub>4</sub> reactants have on air oxidation of PAP<sub>r</sub> to PAP<sub>o</sub> are also explored.

## Experimental Section

**Protein.** Purple acid phosphatase (uteroferin) was obtained from the allantoic fluids of porcine conceptuses at midpregnancy, and purified according to procedures already described.<sup>7,26</sup>

**Tetraoxo Anions.** Sodium molybdate, Na<sub>2</sub>[MoO<sub>4</sub>]·2H<sub>2</sub>O (Sigma), sodium tungstate Na<sub>2</sub>[WO<sub>4</sub>]·2H<sub>2</sub>O (BDH, Analar), sodium orthovanadate, Na<sub>3</sub>[VO<sub>4</sub>] (Sigma), and disodium hydrogen arsenate Na<sub>2</sub>H[AsO<sub>4</sub>]·7H<sub>2</sub>O (Aldrich) were used. At pH < 7 the formation of [HMoO<sub>4</sub>]<sup>−</sup> and [HWO<sub>4</sub>]<sup>−</sup> hydroxo forms initiates oligomerization of [MoO<sub>4</sub>]<sup>2−</sup> and [WO<sub>4</sub>]<sup>2−</sup>. Relevant acid dissociation constants  $K_{1a}$  and  $K_{2a}/M$  are as defined in (4) and (5), where pK<sub>a</sub> (25 °C) values are respectively 3.65



and 3.55 (Mo;  $I = 1.0 \text{ M}$ )<sup>30</sup> and 3.5 and 4.6 (W;  $I = 0.10 \text{ M}$ ).<sup>31</sup> In the latter case it is noted that  $\text{p}K_{2a} > \text{p}K_{1a}$ . Whereas O-atom exchange reactions of the d<sup>0</sup> ions [MoO<sub>4</sub>]<sup>2−</sup> and [WO<sub>4</sub>]<sup>2−</sup> with H<sub>2</sub>O and OH<sup>−</sup> are known to be quite fast,<sup>32</sup> those for PO<sub>4</sub> ions are much slower.<sup>33</sup> In the range of pH explored VO<sub>4</sub> oligomerization is observed.<sup>34</sup> The interconversion of V(V) monomer and dimer forms has been studied by NMR.<sup>35,36</sup> An essential difference is that oligomerization is more pronounced at the higher pH's ≥ 5, and significant amounts of [V<sub>3</sub>O]<sup>3−</sup> are formed with [VO<sub>4</sub>] at levels ≥ 0.20mM. Relevant pK<sub>a</sub>'s are for H<sub>3</sub>VO<sub>4</sub> (3.2) and H<sub>2</sub>VO<sub>4</sub><sup>−</sup> (3.8) at  $I = 0.50 \text{ M}$  (NaClO<sub>4</sub>). In all cases the tendency for oligomerization to occur is minimized by working at

- (27) Aquino, M. A. S.; Sykes, A. G. *J. Chem. Soc., Dalton Trans.* **1994**, 683.  
 (28) Aquino, M. A. S.; Wang, X.-D.; Que, L., Jr.; Sykes, A. G. Unpublished work.  
 (29) Crans, D. C.; Simone, C. M.; Holz, R. C.; Que, L., Jr. *Biochemistry* **1992**, *31*, 11731.  
 (30) Aveston, J. *Inorg. Chem.* **1964**, *3*, 981.  
 (31) Schwarzenbach, G.; Geier, G.; Littler, J. *Helv. Chim. Acta* **1962**, *45*, 2601.  
 (32) von Felton, H.; Wernli, B.; Gamsjäger, H.; Baertschi, P. *J. Chem. Soc., Dalton Trans.* **1978**, 496.  
 (33) Bunton, C. A.; Llewellyn, D. R.; Vernon, C. A.; Welch, V. A. *J. Chem. Soc.* **1961**, 1636.  
 (34) (a) Dyrssen, D.; Sekine, T. *J. Inorg. Nucl. Chem.* **1964**, *26*, 981. (b) Ingri, N.; Brito, F. *Acta. Chem. Scand.* **1959**, *13*, 1971. (c) Newman, L.; La Fleur, W. J.; Brousaides, F. J.; Ross, A. M. *J. Am. Chem. Soc.* **1958**, *80*, 4491.  
 (35) Gresser, M. J.; Tracey, A. S.; Parkinson, K. M. *J. Am. Chem. Soc.* **1986**, *108*, 6229.  
 (36) Crans, D. B.; Rithner, C. D.; Theisen, L. A. *J. Am. Chem. Soc.* **1990**, *112*, 2901.

(25) Sträter N.; Klabunde, T.; Tucker, P.; Witzel, H.; Krebs, B. *Science* **1995**, *268*, 1489.

(26) Aquino, M. A. S.; Lim, J.-S.; Sykes, A. G. *J. Chem. Soc., Dalton Trans.* **1994**, 429.

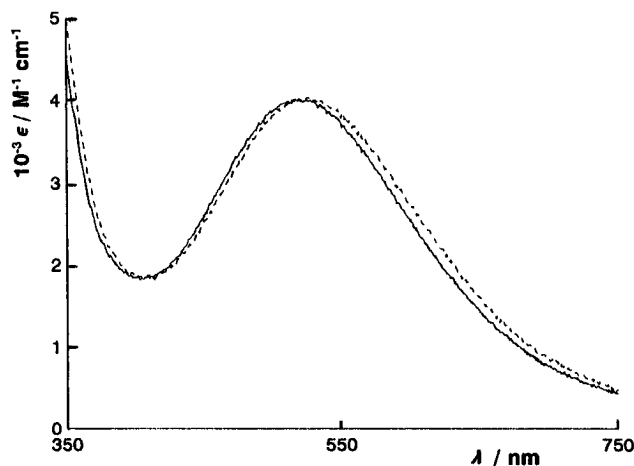
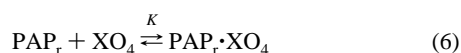


**Figure 2.** UV-vis absorbance spectra for (a) the active  $\text{Fe}^{\text{II}}/\text{Fe}^{\text{III}}$  form of  $\text{PAP}_r$  peak at 515 nm (—), and (b) the molybdate adduct  $\text{PAP}_r \cdot \text{MoO}_4$  peak at 525 nm (- -) formed by addition of molybdate ( $2.8 \times 10^{-4}$  M) to  $\text{PAP}_r$  ( $2.6 \times 10^{-5}$  M) at pH 5.6.

low total  $\text{XO}_4$  concentrations. The dependencies of rate constants on  $[\text{XO}_4]$  were explored at the higher pH of 5.6 compared to 4.6 for the studies with the phosphates.<sup>26</sup> At pH 5.6 “safe” upper limits for  $\text{XO}_4$  were found to be  $1.0 \times 10^{-3}$  M (Mo),  $4.0 \times 10^{-4}$  M (W), and  $2.0 \times 10^{-4}$  M (V). To study the effects of pH concentrations  $1.5 \times 10^{-4}$  M (Mo)  $3.0 \times 10^{-5}$  M (W) and  $1.6 \times 10^{-4}$  M (V) were adopted. Literature  $pK_a$ 's (25 °C) for  $\text{H}_3\text{AsO}_4$  are  $pK_{1a} = 2.24$ ,  $pK_{2a} = 6.94$ , and  $pK_{3a} = 11.50$ , at an ionic strength  $I$  extrapolated to zero.<sup>37</sup> The dominant forms present under the conditions adopted for these studies are accordingly  $[\text{MoO}_4]^{2-}$ ,  $[\text{WO}_4]^{2-}$ ,  $[\text{HVO}_4]^-$ , and  $[\text{H}_2\text{AsO}_4]^-$ , with some tendency for protonation to occur at the lower pH's.

**Formation Constants  $\text{XO}_4$  with  $\text{PAP}_r$ .** Inhibition constants ( $K_i$ ) from the effect of  $\text{XO}_4$  anions on  $\text{PAP}_r$  (uteroferin) phosphate ester hydrolysis, enable formation constants  $K/M^{-1}$  as defined in (6) to be



determined (by taking reciprocals). At pH 4.9 literature  $K/M^{-1}$  values are  $2.5 \times 10^5$  (Mo),  $2.5 \times 10^5$  (W), and 500 (As) and at pH 5.5 are  $2.0 \times 10^5$  (Mo),  $1.4 \times 10^6$  (W), 1562 (As), and  $2.5 \times 10^4$  (V).<sup>7,29</sup> These are more favorable than the corresponding value for phosphate ( $83 M^{-1}$  at pH 4.9), and it was possible therefore to work at lower concentrations. Thus with  $[\text{PO}_4] < 1\text{mM}$  there are no detectable absorbance changes, whereas in the present studies with e.g.  $[\text{WO}_4]^{2-}$  it was possible to use concentrations as low as  $3 \times 10^{-5}$  M.

**Kinetic Studies.** These were carried out at  $25.0 \pm 0.1$  °C, with ionic strength  $I = 0.100 \pm 0.001$  M adjusted using NaCl. Acetate/acetic acid buffer (40mM) was used to vary the pH in the range upto pH 5.8, and Bis/Tris buffer (Sigma) at pH > 5.8. Reactions were monitored at peak positions/nm for the respective products  $\text{PAP}_r \cdot \text{MoO}_4$  (525),<sup>18</sup>  $\text{PAP}_r \cdot \text{WO}_4$  (520),<sup>38</sup>  $\text{PAP}_r \cdot \text{VO}_4$  (520),<sup>39</sup> which compare with  $\text{PAP}_r$  (515). In the case of  $\text{PAP}_r \cdot \text{AsO}_4$  the product peaks at 510 nm.<sup>7</sup> All these peaks have  $\epsilon$  values close to  $4000 M^{-1}\text{cm}^{-1}$ . A Dionex D-110 stopped-flow spectrophotometer was used, and rate constants  $k_{\text{obs}}/s^{-1}$  were evaluated using OLIS programs (Bogart, GA) giving a nonlinear regression fit. In the case of arsenate absorbance changes were not large enough to enable rate constants to be determined. Absorbance changes observed in the case of molybdate are illustrated in Figure 2. In all oxidation studies,  $\text{PAP}_r \rightarrow \text{PAP}_o$ , ethylenediaminetetraacetate (0.10 mM) was added to complex any free Fe ions. This is particularly important at the higher oxyanion concentrations when slight denaturation of the enzyme occurs.

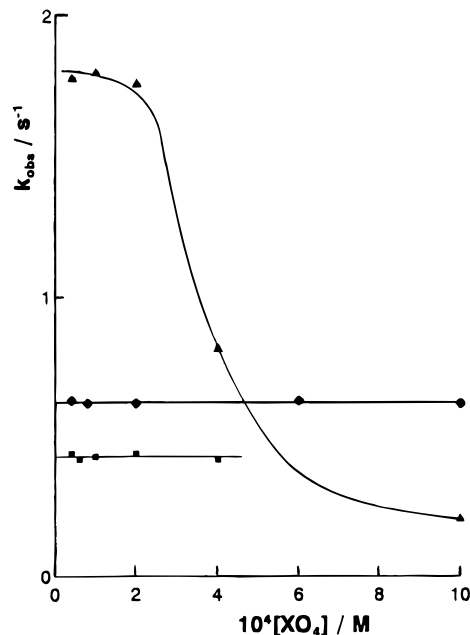


**Figure 3.** First-order rate constants  $k_{\text{obs}}$  (25 °C) for the reaction of the  $\text{Fe}^{\text{II}}/\text{Fe}^{\text{III}}$  form of  $\text{PAP}_r$  (uteroferin) with a given concentration of molybdate  $[\text{MoO}_4]^{2-}$  (●), tungstate(VI)  $[\text{WO}_4]^{2-}$  (■), and vanadate(V)  $[\text{HVO}_4]^{2-}$  (▲) at pH 5.6,  $I = 0.100$  M (NaCl).

**Table 1.** Variation of First-Order Rate Constants (25 °C) for the Reactions of Tetraoxo Anions  $\text{XO}_4$  with Active  $\text{Fe}^{\text{II}}/\text{Fe}^{\text{III}}$   $\text{PAP}_r$  (uteroferin) ( $3.0\text{--}8.0 \times 10^{-6}$  M, at Different pH's,  $I = 0.100$  M (NaCl))

Reaction with Molybdate(VI) ( $1.5 \times 10^{-4}$ M)										
pH	3.88	4.20	4.30	4.45	4.63	4.78	5.10	5.25	5.38	5.60
$k_{\text{obs}}/s^{-1}$	7.7	5.7	3.9	2.5	1.90	1.44	1.09	0.96	0.75	0.62
pH	5.92									
$k_{\text{obs}}/s^{-1}$	0.53									
Reaction with Tungstate(VI) ( $3.0 \times 10^{-5}$ M)										
pH	3.54	3.74	4.10	4.20	4.40	4.62	4.80	5.10	5.38	
$k_{\text{obs}}/s^{-1}$	10.7	9.5	4.0	2.50	1.30	0.99	0.80	0.70	0.51	
pH	5.72									
$k_{\text{obs}}/s^{-1}$	0.38									
Reaction with Vanadate(V) ( $1.6 \times 10^{-4}$ M)										
pH	3.56	3.90	4.20	4.40	4.76	5.20	5.62	6.01		
$k_{\text{obs}}/s^{-1}$	8.4	7.0	4.2	2.33	1.58	1.22	0.79	0.70		

## Results

**Kinetics of  $\text{PAP}_r$  with  $\text{XO}_4$ .** First-order rate constants  $k_{\text{obs}}$  were determined at pH 5.6 with concentrations of  $\text{XO}_4$  as illustrated in Figure 3. No variations in  $k_{\text{obs}}$  are observed in the case of  $\text{MoO}_4$ ,  $k_{\text{obs}} = 0.62 \pm 0.01 s^{-1}$ , or  $\text{WO}_4$ ,  $k_{\text{obs}} = 0.43 \pm 0.02 s^{-1}$ . With vanadate(V) as  $\text{H}_2\text{VO}_4^-$ ,  $k_{\text{obs}} = 1.78 \pm 0.02 s^{-1}$ , but at concentrations  $> 2.0 \times 10^{-4}$  M there is an apparent decrease in  $k_{\text{obs}}$  due to formation of  $[\text{V}_3\text{O}_3]^{3-}$ ,<sup>34</sup> Figure 3.

A listing of rate constants  $k_{\text{obs}}$  with pH in the range 3.5–6.3 is given in Table 1. The variations in rate constants with pH are shown in Figure 4. A single uniphasic decrease is observed in each case with increasing pH, and no additional steps are apparent as in the case of some  $\text{PO}_4$  reactants, which exhibit other protonation equilibria in the pH range studied.<sup>26</sup> The lines drawn in Figures 3 and 4 are to indicate trends and are not computer fits since no quantitative treatment is given.

**Rate Constants for Reaction with  $\text{O}_2$ .** Whereas an equilibrium mix containing  $\text{PAP}_r \cdot \text{PO}_4$  is oxidized more quickly by air than  $\text{PAP}_r$ ,<sup>26</sup> in the case of  $\text{PAP}_r \cdot \text{MoO}_4$  at pH 5.0 no reaction is observed over 24 h. Absorbance changes were monitored at  $\sim 620$  nm. The conditions explored were with  $\text{PAP}_r$  at  $2.65 \times 10^{-5}$  M and  $\text{MoO}_4$  at 0.31 and 0.63 mM. With arsenate on the

(37) Flis, I. E.; Mischchenko, K. P.; Tumanova, T. A. *Russ. J. Inorg. Chem. (Engl. Transl.)* **1959**, *4*, 120.

(38) Vincent, J. B.; Crowder, M. W.; Averill, B. A. *Biochemistry* **1991**, *30*, 3025.

(39) Antanaitis, B. C.; Aisen, P. J. *Biol. Chem.* **1985**, *260*, 751.

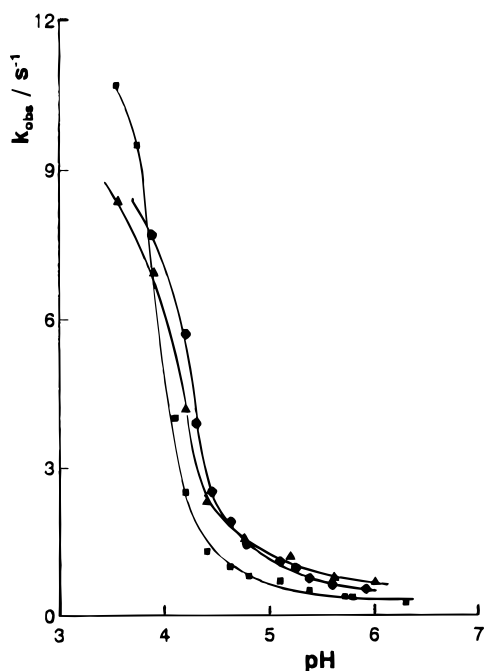


**Figure 4.** Variation of first-order rate constants  $k_{\text{obs}}$  (25 °C) with pH for reactions of the active Fe<sup>II</sup>Fe<sup>III</sup> form of PAP<sub>r</sub> (uteroferrin) with dominant forms of molybdate(VI), [MoO<sub>4</sub>]<sup>2-</sup> (●), tungstate(VI), [WO<sub>4</sub>]<sup>2-</sup> (■), and vanadate(V), [H<sub>2</sub>VO<sub>4</sub>]<sup>-</sup> (▲), I = 0.100 M (NaCl).

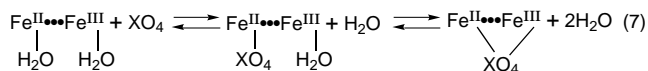
other hand it was found that PAP<sub>r</sub>, AsO<sub>4</sub> is more rapidly air oxidized than PAP<sub>r</sub>. Rate constants  $10^5 k_{\text{obs}}$  obtained at different arsenate [AsO<sub>4</sub>]/mM levels, PAP<sub>r</sub> =  $3.03 \times 10^{-5}$  M and [O<sub>2</sub>] =  $2.64 \times 10^{-4}$  M (air saturated solutions), are as follows: 6.4 (10.1), 6.4 (36.3), and 6.2 (58.2), indicating no dependence on [AsO<sub>4</sub>].

## Discussion

Within the limits imposed by the need to retain monomeric tetraoxo XO<sub>4</sub> ions it has been possible to determine first-order rate constants for the reaction of XO<sub>4</sub> (in excess) with PAP<sub>r</sub> (X = Mo, W, V) and demonstrate that as in the case of PO<sub>4</sub> reactants<sup>26</sup> rate constants are independent of [XO<sub>4</sub>], Figure 3. Thus at pH 5.6 it was possible to use a range of molybdate(VI) concentrations up to  $1.0 \times 10^{-3}$  M, and tungstate(VI) to  $4 \times 10^{-4}$  M, but with vanadate(V) ( $2.0 \times 10^{-4}$  M) more restrictive conditions were necessary to avoid formation of [V<sub>3</sub>O<sub>9</sub>]<sup>3-</sup>. Absorbance changes in the case of X = As were too small for rate constants to be determined. It was also possible to vary the pH within the range 3.5–6.3, while retaining mononuclear species, Figure 4. The mononuclear ions which are relevant are [MoO<sub>4</sub>]<sup>2-</sup>, [WO<sub>4</sub>]<sup>2-</sup>, and [H<sub>2</sub>VO<sub>4</sub>]<sup>-</sup>, respectively. The pH at the lower limit was restricted to 3.5 for Mo(VI) and >4.0 for W(VI).

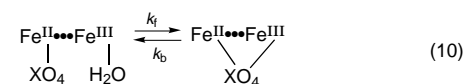
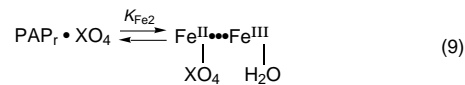
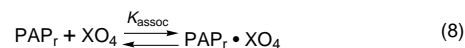
The mammalian Fe<sup>II</sup>Fe<sup>III</sup> form of PAP<sub>r</sub> has properties in common with the Zn<sup>II</sup>Fe<sup>III</sup> enzyme, Figure 1. In particular the H<sub>2</sub>O coordinated to each metal is an important feature. A step involving acid dissociation of Fe(III)-H<sub>2</sub>O has been suggested,<sup>23,26</sup> in order to explain the decrease in rate constants with increasing pH. Support comes from the observation that, e.g., coordinated and uncoordinated [H<sub>2</sub>PO<sub>4</sub>]<sup>-</sup> do not undergo deprotonation in this range of pH, and therefore the effect of pH must originate from the protein. There are alternative explanations, but if there is an H<sub>2</sub>O coordinated to the Fe<sup>III</sup>, it would be expected to exhibit acid behavior in this range. With vanadate(V) at  $\leq 5 \times 10^{-4}$  M, the protonated form [H<sub>3</sub>VO<sub>4</sub>] is dominant at pH's 3.2–3.8 and [H<sub>2</sub>VO<sub>4</sub>]<sup>-</sup> from 3.8 to 7.8, and this may contribute alongside Fe(III)-OH and Fe(III)-H<sub>2</sub>O

equilibration to the trends observed for VO<sub>4</sub> in Figure 4. In the previous studies with phenyl phosphate, pyrophosphate, tripolyphosphate and ATP, a second pH effect was clearly apparent suggesting that the degree of protonation of the Fe(II)-coordinated XO<sub>4</sub> may also be relevant.<sup>26</sup> In all other respects the kinetics reported in this paper are similar to those observed for [H<sub>2</sub>PO<sub>4</sub>]<sup>-</sup>,<sup>26</sup> and the mechanism can be expressed as in (7). Octahedral high-spin aqua Fe<sup>II</sup> is  $10^2$ – $10^3$  times more



labile than the corresponding aqua Fe<sup>III</sup> consistent with these changes.<sup>26</sup> The observation that trimethyl phosphate, with only one oxo group, does not appear to react at the Fe<sup>III</sup>, but inhibits reaction with [H<sub>2</sub>PO<sub>4</sub>]<sup>-</sup>, supports a mechanism in which the initial change is at the Fe<sup>II</sup>.<sup>26</sup> The second equilibrium is we believe important in determining the kinetic behavior observed. In addition to Fe(III)-OH formation, protonation/deprotonation of XO<sub>4</sub> would be expected to contribute if monodentate XO<sub>4</sub> and  $\mu(\text{XO}_4)$  forms exhibit different degrees of protonation in the range of pH explored. Since only one process is apparent in the pH profiles in Figure 4 the behavior is like that of [H<sub>2</sub>PO<sub>4</sub>]<sup>-</sup> and simpler than in the case of the other phosphates.<sup>26</sup>

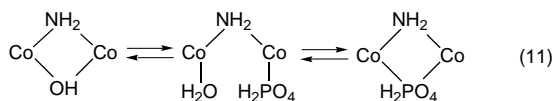
With these additional studies it is clear that all the reactions so far studied are independent of [XO<sub>4</sub>] and that this is not a special feature of the PO<sub>4</sub> reagents. The sequence in (7) can explain the independence of [XO<sub>4</sub>] if  $K$  values for the first stage are large so that  $K[\text{XO}_4] \gg 1$ . The extent of formation of ( $\mu\text{XO}_4$ ) products in the second stage of (7), gives rise to the different inhibition effects referred to in the experimental section. From redox studies on the oxidation of PAP<sub>r</sub> with [Fe(CN)<sub>6</sub>]<sup>3-</sup>,<sup>27</sup> saturation kinetics apply and  $K = 540 \text{ M}^{-1}$  for association of the oxidant to PAP<sub>r</sub> prior to electron transfer. Moreover redox-inactive complexes [Cr(CN)<sub>6</sub>]<sup>3-</sup> ( $K = 550 \text{ M}^{-1}$ ) and [Mo(CN)<sub>8</sub>]<sup>4-</sup> ( $K = 1580 \text{ M}^{-1}$ ) inhibit the [Fe(CN)<sub>6</sub>]<sup>3-</sup> reaction and provide further evidence for electrostatically controlled association steps as a part of these studies. There is therefore at least one favorable site for association of anionic reactants within electron-transfer range of the active site of PAP<sub>r</sub>. The initial association step can be included in the mechanism to give (8) – (10), where (8) and (9) together give extensive complexation.



It is proposed that H-bonding as well as overall charge contribute to (8) to account for the favorable nature of the interaction. The overall equilibrium constant for (8) – (10) can be expressed as  $K_{\text{assoc}} K_{\text{Fe2}} K_{\text{Fe3}}$ , where  $K_{\text{Fe3}} = k_f/k_b$ . The rate constant  $k_{\text{obs}}$  has forward  $k_f K_{\text{assoc}} K_{\text{Fe2}}$  and reverse  $k_b$  components.

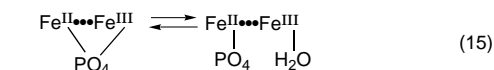
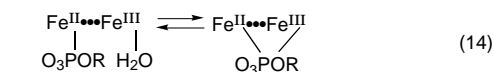
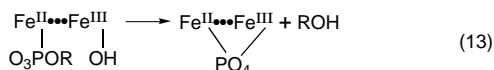
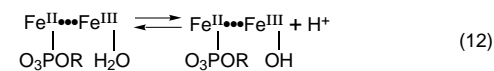
The reaction which models most closely the formation of a  $\mu$ -phosphato product is that involving the interconversion of [NH<sub>3</sub>]<sub>4</sub>Co $\mu$ (NH<sub>2</sub>OH)Co(NH<sub>3</sub>)<sub>4</sub><sup>4+</sup> and [(NH<sub>3</sub>)<sub>4</sub>Co $\mu$ (NH<sub>2</sub>, H<sub>2</sub>-PO<sub>4</sub>)Co(NH<sub>3</sub>)<sub>4</sub>]<sup>4+</sup> in the presence of H<sup>+</sup>/[H<sub>2</sub>PO<sub>4</sub>]<sup>-</sup>, as indicated in (11).<sup>40</sup> Similar reactions of other tetraoxo and related anions

(40) Edwards, J. D.; Foong, S-W.; Sykes, A. G. *J. Chem. Soc., Dalton Trans.* **1973**, 829.



have been reported.<sup>41</sup> Both equilibria in (11) are rapid for substitution at Co(III), and no buildup of the intermediate was detected. The close proximity of ligands involved in bridge closure accounts for the faster rate processes.

In order to account for phosphatase activity the mechanism (12)–(15) is proposed. In this mechanism conjugate-base formation in (12) leads to hydrolysis of the O<sub>3</sub>P(OR)<sup>2-</sup> ester in (13), but no similar hydrolysis is proposed for (14). Rate



constants  $k_{\text{obs}}$  for [H<sub>2</sub>PO<sub>4</sub>]<sup>-</sup>, [MoO<sub>4</sub>]<sup>2-</sup>, [WO<sub>4</sub>]<sup>2-</sup>, and [H<sub>2</sub>VO<sub>4</sub>]<sup>-</sup> show little variation and are in the range 7–12 s<sup>-1</sup> at pH ~3.5.

(41) (a) Foong, S.-W.; Sykes, A. G. *J. Chem. Soc., Dalton Trans.* **1973**, 504, (b) Edwards, J. D.; Yang, C.-H.; Sykes, A. G. *J. Chem. Soc., Dalton Trans.* **1974**, 1561.

This suggests that the rate controlling process for  $k_f$  in (10) maybe loss of an H<sub>2</sub>O from the Fe(III). At pH 4.9, which corresponds to maximum enzyme activity, (13) will be at its most effective and rate constants  $k_{\text{obs}}$  for the different XO<sub>4</sub>'s are also in a narrow range 0.50–1.44 s<sup>-1</sup>. This is surprising in view of the different labilities of XO<sub>4</sub> anions,<sup>32,33</sup> suggesting that some other process may be rate determining and that a further elaboration may be required. One possibility is that equilibration rate constant equal to  $k_f + k_b$  may be effective with  $k_b$  rather than  $k_f$  dominant. Unfortunately there is insufficient information at present to quantify  $k_f$  and  $k_b$  separately.

Finally the reactivity of PAP<sub>r</sub>·XO<sub>4</sub> adducts with O<sub>2</sub> at pH 5.0 is accounted for by the different reduction potentials (vs nhe). The latter have been determined for the PAP<sub>o</sub>/PAP<sub>r</sub> couple (367 mV) and for PAP<sub>r</sub> adducts with PO<sub>4</sub> (183 mV), and AsO<sub>4</sub> (262 mV).<sup>18</sup> In the studies with AsO<sub>4</sub> the kinetics are independent of [AsO<sub>4</sub>] indicating complexing prior to reaction with O<sub>2</sub>. Rate constants for the O<sub>2</sub> reaction with PAP<sub>r</sub>·AsO<sub>4</sub> ( $6.3 \times 10^{-5} \text{ s}^{-1}$ ) and PAP<sub>r</sub>·PO<sub>4</sub> ( $6.8 \times 10^{-5} \text{ s}^{-1}$ )<sup>26</sup> are very similar. The reduction potential in the presence of MoO<sub>4</sub> is high at 498 mV (pH 6.01) and no reaction of PAP<sub>r</sub>·MoO<sub>4</sub> with O<sub>2</sub> was observed over ~24 h. Whereas MoO<sub>4</sub> and WO<sub>4</sub> bind tightly to PAP<sub>r</sub>, phosphate and arsenate bind more weakly, which may facilitate O<sub>2</sub> access.<sup>14</sup>

**Acknowledgment.** We thank the UK Science and Engineering Research Council (J.-S.L.) and Nato/National Sciences and Engineering Research Council of Canada (M.A.S.A.) for post-doctoral support.

IC9501390